Journal Pre-proof

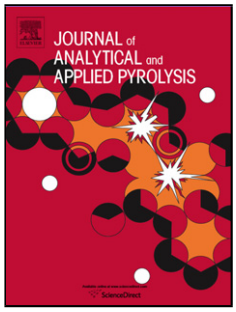

The role of catalyst acidity and shape selectivity on products from the catalytic fast pyrolysis of beech wood

Joseph Socci, Alireza Saraeian, Stylianos D. Stefanidis, Scott W. Banks, Brent H. Shanks, Tony Bridgwater

PII: S0165-2370(19)30408-5

DOI: https://doi.org/10.1016/j.jaap.2019.104710

Reference: JAAP 104710

To appear in: *Journal of Analytical and Applied Pyrolysis*

Received Date: 31 May 2019

Revised Date: 19 September 2019

Accepted Date: 9 October 2019

Please cite this article as: Socci J, Saraeian A, Stefanidis SD, Banks SW, Shanks BH, Bridgwater T, The role of catalyst acidity and shape selectivity on products from the catalytic fast pyrolysis of beech wood, *Journal of Analytical and Applied Pyrolysis* (2019), doi: https://doi.org/10.1016/j.jaap.2019.104710

The role of catalyst acidity and shape selectivity on products from the catalytic fast pyrolysis of beech wood

Joseph Socci[1], Alireza Saraeian[2,3], Stylianos D. Stefanidis[1], Scott W. Banks[1], Brent H. Shanks[2,3], Tony Bridgwater[1*]

1. European Bioenergy Research Institute (EBRI), School of Engineering and Applied Science, Aston University, Aston Triangle, Birmingham, B4 7ET, United Kingdom.
   *Corresponding Author: a.v.bridgwater@aston.ac.uk
2. Department of Chemical and Biological Engineering, Iowa State University, Ames, IA 50011, USA
3. NSF Engineering Research Centre for Biorenewable Chemicals (CBiRC), Ames, IA 50011, USA

Graphical abstract

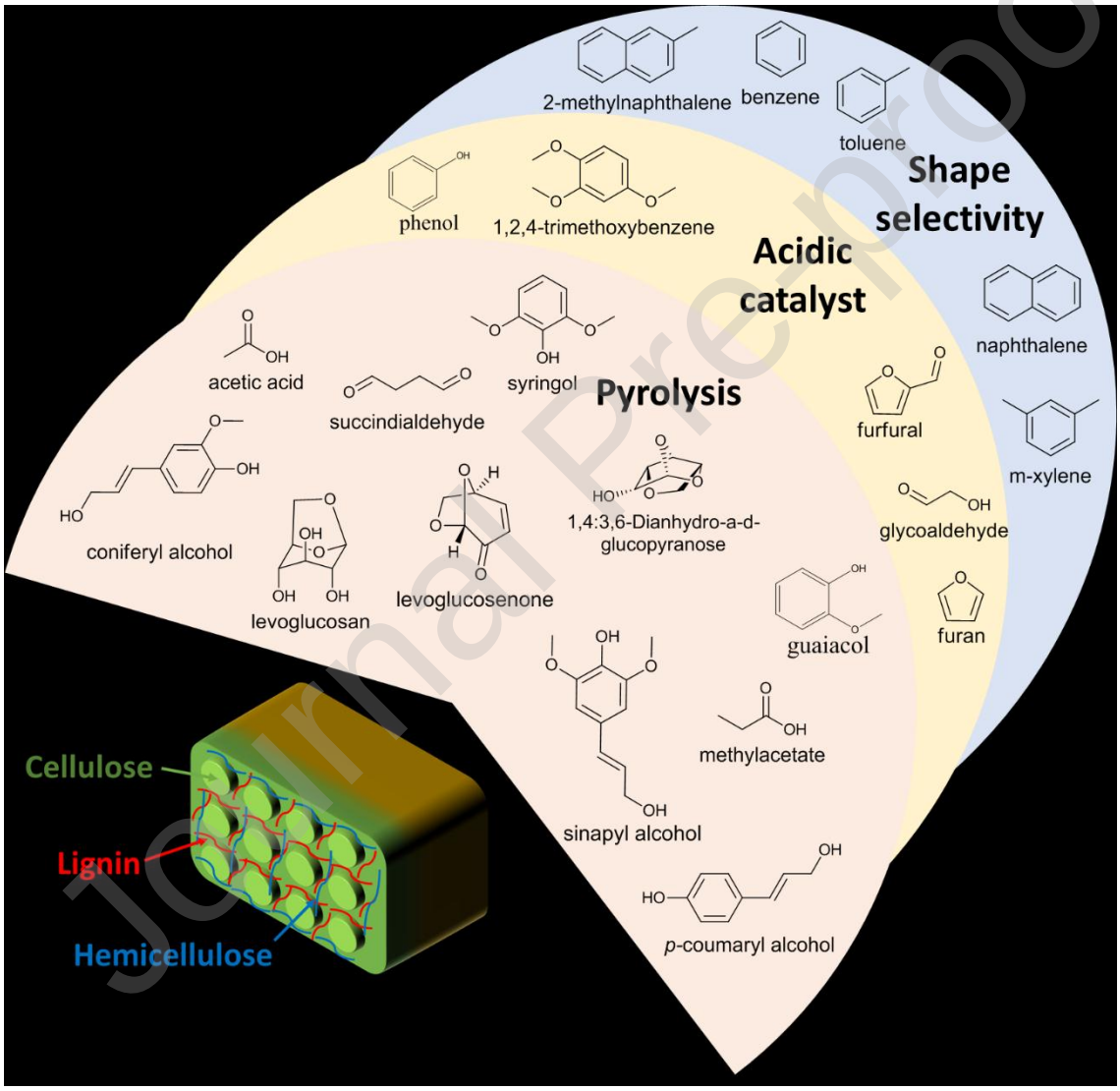

Highlights

{ { Synthesis of mesoporous Al-SBA-15 catalyst with similar acidity to ZSM-5.

{ { Testing of high acidity Al-SBA-15 in comparison to ZSM-5 for CFP of beech wood.

- Solid acid catalysts initially followed similar reaction pathway.
- Shape selectivity of ZSM-5 directed selectivity towards aromatic production.
- Mesoporous Al-SBA-15 lacked shape selectivity and formed more coke.

Abstract

The catalytic fast pyrolysis (CFP) of biomass represents an efficient integrated process to produce deoxygenated stable liquid fuels and valuable chemical products from lignocellulosic biomass. The zeolite ZSM-5 is a widely studied catalyst for the CFP process. However, its microporous structure may limit the diffusion of high molecular weight pyrolysis intermediates to its active sites. Mesoporous aluminosilicates such as Al-SBA-15 are promising materials with larger pore sizes that can overcome these diffusional limitations. Previous comparisons between mesoporous aluminosilicates and ZSM-5 for the CFP process have neglected the disproportionately high acidity of ZSM-5. In this study, an Al-SBA-15 catalyst has been synthesised with high acidity, comparable to that of a ZSM-5 catalyst with a Si:Al ratio of 15:1. The synthesised Al-SBA-15 catalyst was characterised by N_2 physisorption, XRD and propylamine-TPD, and was compared to a ZSM-5 catalyst and a typical industrial equilibrium fluid catalytic cracking catalyst (e-FCC). All three catalysts were used at three different catalyst to biomass (C/B) ratios, to investigate the effect of varying concentrations of acid sites on the product distribution from the catalytic fast pyrolysis of beech wood. Interestingly, despite their dissimilar structural architectures, all three solid acid catalysts displayed similar reaction pathways towards the cracking of high molecular weight products such as levoglucosan and formation of intermediates including phenolics and furans. However, the selectivity towards the final catalytic products was dictated mainly by the structure of the catalysts. Despite their very similar surface area and acidity, the ZSM-5 exhibited high selectivity for the formation of desirable aromatic hydrocarbon products due to its shape-selective micropore structure, while Al-SBA-15 instead shifted the selectivity towards the formation of undesirable coke. The results highlighted the importance of catalyst shape-selectivity in the catalytic fast pyrolysis of biomass for the conversion of pyrolysis vapours into desirable products and the suppression of undesirable solid byproduct formation.

Keywords: Analytical pyrolysis; Catalytic fast pyrolysis; Zeolite; Mesoporous materials; Biomass

1 Introduction

The conversion of biomass into fuels and chemicals has been of growing interest by industry, governments and the scientific community over the past 40 years [1]. Biomass is the only source of non-gaseous renewable carbon and is abundant worldwide. Growing concerns surrounding energy security, and the environmental effects of large-scale fossil fuel consumption, will lead to the increased utilisation of biomass resources in the coming years.

Fast pyrolysis of biomass is a thermochemical conversion process that can convert solid biomass into a pyrolysis liquid (bio-oil), non-condensable gas products and solid char (biochar). The fast pyrolysis process involves the rapid heating of biomass to high temperatures (400-600 °C) in the absence of oxygen. This thermally deconstructs the complex biopolymer components of biomass, forming pyrolysis vapours. Subsequent rapid cooling of the evolved vapours (hot vapour residence times <2 s) inhibits secondary cracking and polymerisation reactions to minimise gas and solid phase products and maximise liquid yields [2].

Much of the focus of biomass fast pyrolysis has been on the production of fuels and chemicals [3,4]. The main liquid product (bio-oil) is a complex mixture of water and over 400 oxygenated compounds derived from the thermal decomposition of the biomass feedstock [5,6]. Bio-oil has higher energy density than biomass and is easier to transport and handle. However, bio-oil is characterised by a series of undesirable properties, such as immiscibility with hydrocarbon fuels, low calorific value, corrosivity to common, as well as instability and proneness to aging, which make its storage, transportation and processing into transportation fuels and chemicals, challenging [7]. These undesirable properties have been attributed to the reactive oxygenates it contains and in general to its high oxygen content (35-40 wt. %) [2]. For these reasons, bio-oil is considered a low-quality product and several strategies have been investigated for its upgrading, in order to facilitate processing into transportation fuels and high added value chemical products.

Bio-oil upgrading strategies focus on the reduction of its oxygen content and reactive components. Post-pyrolysis upgrading processes such as catalytic cracking and hydrodeoxygenation, have been investigated by many groups [8,9], though processing can be challenging due to the instability of the bio-oil. Catalytic fast pyrolysis (CFP) is a process for the one-step production of an improved-quality liquid product (catalytic bio-oil) from biomass pyrolysis. CFP involves the fast pyrolysis of biomass in the presence of a heterogeneous catalyst, either in-situ (catalyst in contact with biomass) or ex-situ (no contact between biomass and catalyst). The vapours released from biomass react on the catalyst surface and reactive oxygenates are converted into more stable products, while oxygen is removed in the form of CO_2, CO and water. As a result, a partially deoxygenated bio-oil is produced, which is more energy dense, less corrosive and has improved stability compared to thermal bio-oil. Due to its

improved properties, catalytic bio-oil can be more readily upgraded to drop-in biofuels and bio-based commodity chemicals utilizing downstream processes [10t 12]. On the downside, the yield of the organic bio-oil is substantially reduced due to the removal of oxygen, as well as due to carbon losses from the formation of byproducts such as catalytic coke and non-condensable gases. As such, the design and selection of suitable catalysts is crucial for the efficient deoxygenation of the pyrolysis vapours, the minimization of undesirable byproducts, the selective formation of high added value chemicals and by extension, the economic feasibility of the process.

Solid acid catalysts such as zeolites, metal oxides and mesoporous aluminosilicates (for example ZSM-5, zinc oxide, magnesium oxide, silica-alumina and Al-MCM-41), have been studied for the catalytic pyrolysis of biomass [13t 18]. The acidity of the catalyst, particularly Brønsted acidity, is critical for cracking oxygenates in the pyrolysis vapours. Theoretically, the cracking activity of the solid acid catalyst is proportional to its acidity [14]. The addition of a catalyst to the process increases the complexity due to the need to consider both fast pyrolysis variables and the catalytic process variables. The product distribution can be manipulated by varying the fast pyrolysis variables such as heating rate and reaction temperature, as well as the properties of the catalyst, catalyst to biomass ratio (C/B) and residence time of the vapours across the catalyst bed [19].

The ZSM-5 zeolite is the most widely studied catalyst for the CFP of biomass. It possesses high acidity and it has been shown to be highly selective for the production of aromatic hydrocarbons due to its three-dimensional shape-selective micropore system with pore diameters ca. 0.5 nm [20]. However, its microporous structure also limits the diffusion of large pyrolysis intermediates to the internal pores of the zeolite, where a large proportion of the catalytically active acid sites are located. For this reason, mesoporous materials such as Al-MCM-41 and Al-SBA-15 with larger pore sizes (2-10 nm) have been considered to address the challenge of cracking high MW molecules. Al-MCM-41 and Al-SBA-15 are structurally similar, however, Al-SBA-15 offers several advantages over Al-MCM-41, such as larger pore sizes and increased hydrothermal stability owing to thicker pore walls [21].

Previous research by Adam et al. [22], on the CFP of spruce wood with Al-MCM-41 and Al-SBA-15, concluded that use of these catalysts resulted in an increased concentration of desirable compounds in the bio-oil; compounds such as hydrocarbons, alcohols and phenolics were increased, while the concentration of less desirable compounds such as organic acids and carbonyls was decreased compared to non-catalytic CFP. Similar findings were presented by Jeon et al. [23] on the CFP of biomass components over mesoporous SBA-15 catalysts. It was claimed that the quality of oil increased in terms of decreased acidity and increased aromatic content using Al-SBA-15 compared to non-catalytic pyrolysis and SBA-15. The improvement in oil quality was attributed to the increased acidity of the Al-SBA-15 catalyst compared to SBA-15. A more in-depth assessment was performed by Custodis et al. [24], on the CFP of lignin with a variety of mesoporous aluminosilicates and zeolites,

including ZSM-5, Al-MCM-41 and Al-SBA-15. The results concluded that a complex relationship exists between the product distribution and the catalyst properties, such as pore size, number of acid sites and pore connectivity. The enhanced shape selectivity of ZSM-5 to aromatics was also observed. Lu et al. [25,26] compared the catalytic cracking of biomass pyrolysis vapours over Al-SBA-15 catalysts and zeolitic ZSM-5 and HY catalysts. They reported that SBA-15 catalysts favoured the formation of furan, furfural and other oxygenates, while the zeolitic catalysts was more effective for the production of high yields of hydrocarbons. Yaman et al. [27] also compared the catalytic activity of ZSM-5 and Al-SBA-15 and observed in both cases a decreased yield of the organic fraction of the bio-oil. However, ZSM-5 was highly selective towards aromatic hydrocarbons. On the other hand, Al-SBA-15 produced almost no aromatics, while the yields of phenolics, aldehydes and ketones and most significantly coke were all increased. This resulted in both the loss of carbon in the desirable products and catalyst deactivation.

Based on the literature above, it is evident that mesoporous aluminosilicates offer an improvement of liquid quality compared to non-catalytic pyrolysis but the microporous ZSM-5 is a superior catalyst for the formation of more valuable aromatic hydrocarbon products, as well as for the minimization of coke formation. However, as previously mentioned, the catalytic activity of solid acid catalysts is largely determined by their acidic properties. Previous comparisons between ZSM-5 and mesoporous aluminosilicates (Al-MCM-41 and Al-SBA-15) in the CFP of biomass utilized mesoporous aluminosilicates with acidity significantly lower than that of typical ZSM-5 zeolites [22t 24,27]. Aluminium is typically introduced into the structure of SBA-15 using a direct synthesis method which deposits aluminium on the surface of the catalyst. This results in low amounts of aluminium in a tetrahedral environment which is essential for the generation of strong Brønsted acidity, as seen in zeolites. Therefore, the previously reported inferior performance of the mesoporous aluminosilicates could also be attributed to their low acidity and not simply due to the difference in pore size and structure.

In this study, an enhanced aluminium incorporation strategy was used for the synthesis of a highly acidic Al-SBA-15, as a simple yet effective approach to obtain high contents of Al in the tetrahedral environment, generating acidity similar to zeolites. The newly created mesoporous Al-SBA-15 catalyst was used in the catalytic pyrolysis of beech wood and compared to a commercially available ZSM-5 zeolite. The pyrolysis experiments were carried out using a Frontier labs tandem micro-pyrolysis unit attached to a gas chromatograph equipped with a mass spectrometer (MS), a thermal conductivity detector (TCD) and a flame ionization detector (FID). The experimental setup allowed for both the identification and quantification of the major products. Although this experimental set-up may not fully [illegible] CFP of biomass at the

industrial scale, the micro-pyrolysis unit has been used a convenient tool by many research groups to evaluate prospective catalysts with high accuracy [28,29].

The properties of the catalysts such as acidity and porosity were measured to investigate their influence on the product distribution and composition. A commercial equilibrium FCC catalyst (e-FCC) with lower acidity, containing FAU zeolite as the active component, was also used for the CFP of beech wood to investigate product formation at lower catalyst acidities. It is also an industrially relevant catalyst employed for the catalytic conversion of heavy petroleum feedstocks. Furthermore, the experiments were carried out at three different catalyst to biomass (C/B) ratios, 1:1, 5:1 and 10:1, in order to investigate the product distribution and catalyst selectivity across varying concentrations of acid sites. The high C/B ratio of 10:1 was employed to ensure adequate conversion considering the short residence time of the micro-pyrolysis unit (<2 s) compared to fluidised bed reactors (2-10 s) [30,31]. In addition, these C/B ratios are in the range often employed in the fluid catalytic cracking (FCC) process, where generally a catalyst to feed ratio at the bottom of the riser is typically 5.5 [32]. The catalytic pyrolysis experiments were carried out at 500 ºC in order to maximise volatile organic products, thereby minimising thermal effects [2].

2 Materials and methods

2.1 Feedstock characterisation

Beech wood (fagus sylvatica) purchased from J. Rettenmaier & Sohne GmbH + Co. KG, Rosenberg, Germany was used as biomass feed in this work. The beech wood sample was ground and sieved to a particle size range of 100-150 µm. Analysis of the ash content of the beech wood sample was carried out using the ASTM E1755-01 method. Elemental analysis of carbon, hydrogen, nitrogen and sulphur (CHNS) on a wt. % dry ash-free basis was determined using a ThermoScientific Flash 2000 CHNS-O analyser. Oxygen content was estimated as the percentage difference after consideration of the ASTM ash content. For the proximate analysis, approximately 10 mg of beech wood sample was characterised by thermogravimetric analysis using a Perkin-Elmer Pyris 1 TGA. Heating was programmed from 50 °C to 900 °C at 10 °C min^{-1} under a nitrogen flow rate of 20 ml min^{-1}. The heating value of the beech wood feedstock was measured experimentally using an IKA C 1 static jacket oxygen bomb calorimeter.

2.2 Catalyst synthesis and characterisation

The FCC catalyst used in this study was a commercial equilibrium FCC catalyst and is denoted e-FCC. A ZSM-5 zeolite in the ammonia form was purchased from Alfa Aesar with a Si:Al ratio of 15:1. The ZSM-5 was converted to the H form by calcination in air at 575 °C for 6 hours at a heating rate of 2 °C min^{-1}.

An Al-SBA-15 catalyst was prepared using a modified two-step [illegible], to produce a catalyst with a low Si:Al ratio of 5:1 and high acidity, similar to that of ZSM-5. This method was developed by Wu and co-workers [33], using $Al(NO_3)_3\ 9H_2O$ as the aluminium source. Four grams of Pluronic P123 triblock copolymer, used as the pore-directing agent, was dissolved in 125 ml of 2 M HCl solution and stirred at 35 °C for 4 hours. Tetraethyl orthosilicate was used as the silica source (8.5 ml) and was added dropwise and stirred for 3 hours. Then, 3 g of $Al(NO_3)_3 \tilde{} 9H_2O$ was added to the mixture to give the desired Si:Al ratio of 5:1 and stirred for 20 hours. The resulting gel was heated at 100 °C for 48 hours before being cooled to room temperature. The pH value of the mixture was increased to 7.5 by the dropwise addition of 4 M NH_4OH under stirring. The mixture was then subjected to a second hydrothermal treatment at 100 °C for 72 hours. This longer hydrothermal treatment step was to increase pore size [34]. The solid product was separated by vacuum filtration, washed with water, and dried at 60 °C before calcination in air at 550 °C for 6 hours at a ramp rate of 1.5 °C min^{-1}.

Nitrogen physisorption analyses were performed at -196 °C using a Quantachrome Nova 1000 porosimeter and analysed using NovaWin software. Samples were degassed under vacuum at 250 °C for two hours prior to analyses. Surface areas (SA) were calculated using the Brunauer, Emmet and [illegible] a and micropore volume. The total pore volumes were calculated using the Barrett, Joyner and Halenda (BJH) method at the recorded relative pressure of 0.98 in the desorption branch. The BJH method was also applied to the adsorption branch at relative pressures between 0.02 and 0.20 to calculate the mean pore sizes.

Wide angle X-ray diffraction patterns were recorded on a Bruker D8 Advance diffractometer fitted [illegible] -ray diffraction pattern was recorded for Al-SBA-15 in order to display the shape and uniformity of the pore structure.

Catalyst acidity was determined using [illegible] method [35] of propylamine temperature programmed desorption (TPD), where Brønsted acid sites catalyse the decomposition of propylamine through the Hofmann elimination reaction to propene and ammonia. The desorption temperature of the formed propene is inversely proportional to the strength of the acid site. Prior to analyses, propylamine was added dropwise to 100 mg of catalyst sample until saturation. Excess propylamine was removed by drying the sample under vacuum at 35 °C overnight. Temperature programmed desorption was then performed using a Mettler Toledo TGA/DSC 2 StarSystem between 40 and 800 °C under a nitrogen flow of 40 ml min^{-1} and at a ramp rate of 10 °C min^{-1}. Propylamine was converted to propene and ammonia, which were detected using a Pfeiffer Vacuum, ThermoStar MS at m/z = 41 and 17, respectively. The total acidity was subsequently calculated from the moles of adsorbed propylamine

derived from the mass loss in the temperature region where propene and ammonia formation were detected.

2.3 Experimental procedure

Catalytic fast pyrolysis experiments were carried out using a Frontier Labs single-shot tandem micropyrolysis system (Rx-3050tr, Fig. 1). The system contained an independently temperature-controlled quartz pyrolysis tube reactor (4.7 mm ID, 114 mm length). The temperature of the interface between the reactor and the GC inlet was set at 350 °C to prevent premature condensation of pyrolysis products. The biomass sample (approx. 0.3 µg) was first weighed into a deactivated stainless-steel sample cup. Then the required amount of catalyst was added to the sample cup and thoroughly mixed to achieve the required C/B ratio (either 1, 5 or 10). Finally, a small amount of quartz wool was added to prevent any escape of solid particles. The sample cups were purged with helium for approximately 5 min and then dropped into the pyrolysis reactor. Helium was used as a carrier gas (120 ml min^{-1}) to transport the volatile products through the reactor system to the connected GC for online-analysis.

Fig. 1. Schematic diagram of the Frontier Labs tandem micro-pyrolysis reactor-GC-MS/FID/TCD system used in this work. Reproduced from reference [28].

The pyrolysis products were analysed by an Agilent gas chromatograph (Agilent 7890B) equipped with two Agilent medium polarity 1701 columns (Agilent VF1701 ms, 60 m x 250 µm x 0.25 µm) to separate the condensable compounds. The injector was maintained at 270 °C with a split ratio of 42:1 and a carrier gas flow of He set to 120 ml min^{-1}. The GC oven was programmed to start at 35 °C for 7.5 min and then the temperature was ramped to reach 300 °C at a rate of 10 °C min^{-1}. Products were identified using a coupled mass spectrometer (Agilent 5977A). The mass spectrometer was equipped with an Electron Ionisation (EI) source and scanned over the mass range of 15 to 350, with a step size of 0.1 and a frequency of 4.2 scans sec^{-1}. Identified products were quantified using an FID. Light gases and

hydrocarbons were separated using a GasPro column (Agilent GS-GasPro) and quantified using a TCD. Representative GC chromatograms are presented in the supporting information for the non-catalytic (Fig. S2) and catalytic (Fig. S3, S4 and S5) fast pyrolysis experiments.

A set of calibration curves were produced using standard solutions comprised of 35 biomass pyrolysis compounds (see supporting information, Table S1), representing a range of the most abundant pyrolysis products. A total of 60 compounds were quantified assuming the same response factors for structurally similar compounds. All standards were purchased from Sigma-Aldrich. Instead of sample cups, a syringe was used for the introduction of liquid and gas standards into the micro-reactor through a septum. The calibration curves produced linear correlations with coefficient of determination (R^2) values exceeding 0.99. The product yields are presented on a carbon basis [36], which was defined as:

Eq. 1: ; E A H P @ ; L Ö Ô å Õ ä â æ ã å â × è Ö ç / Ö Ô å Õ ä â æ ä å Ø Ô Ö ç Ö Ø ç × T s r r ¨

Char/coke yields were calculated by pyrolysis at 500 °C using a known amount of beech wood (ca. 0.5 mg) and catalyst (corresponding to the desired C/B ratio). The mass of the samples was recorded before and after pyrolysis using a microbalance. The mass difference was considered to be volatile components, while the remaining mass minus the catalyst mass was assumed to be all carbon and was reported as char/coke. All calculations were on a biomass dry ash free basis.

3 Results and discussion

3.1 Feedstock characterisation

The results of the ultimate and proximate analyses, as well as the higher heating value, are given in Table 1. Beech wood was used as a representative hard wood feedstock. The results in Table 1 show that the beech wood had a high oxygen content (50 wt. %) and relatively low ash content (< 1 wt. %), both of which are typical values for wood biomass feedstocks.

Table 1. Elemental and compositional analysis of beech wood.

	Beech wood
Ultimate analysis (wt. %$^{(d.a.f)}$)	
C	44.1
H	6.3
N	0.2
S	0.0
O by difference	49.4
Proximate analysis (wt %$^{(d.b)}$)	
Moisture	4.7
Volatile matter	87.6
Fixed carbon	8.0

ASTM ash content	0.8
Higher heating value (MJ kg^{-1})	19.5

d.a.f. = dry ash free. d.b. = dry basis

3.2 Catalyst characterisation

The XRD patterns of the catalysts, shown in Fig. 2, exhibited the crystalline nature of the e-FCC and ZSM-5 materials. In addition, the diffraction pattern of the e-FCC catalyst is consistent with the planes of FAU type zeolite that it contains. The XRD taken in the low-angle region of the Al-SBA-15 materials shows one intense peak attributed to the (1 0 0) plane and two lower-intensity peaks attributed to the (1 1 0) and (2 0 0) planes, characteristic of well-ordered two-dimensional hexagonal structures [34].

Fig. 2. X-ray diffraction patterns of e-FCC, Al-SBA-15 and ZSM-5 catalysts (Al-SBA-15, in inset, was measured in low angle region).

The nitrogen physisorption isotherms are presented in Fig. 3. The isotherm of e-FCC was characterised as a type IV isotherm, indicative of mesoporous solids and is associated with capillary condensation taking place in the mesopores [37]. The corresponding hysteresis loop was classified as being H4 type. H4 hysteresis loops are associated with particles with internal voids of irregular shape and broad size distribution. This was attributed partly to interparticle mesoporosity and partly to the mesoporosity of the non-zeolitic catalyst phase [38,39].

Fig. 3. N_2 physisorption isotherms for e-FCC, Al-SBA-15 and ZSM-5 catalysts.

The surface and porous properties of all catalysts are presented in Table 2. The BET surface area of the ZSM-5 catalyst was 420 m^2 g^{-1}, which is typical for a ZSM-5 zeolite and within the range of the manufacturer stated values [40]. The Al-SBA-15 catalyst had a very similar surface area of 414 m^2 g^{-1}. Al-free SBA-15 materials typically have surface areas of ca. 800 m^2 g^{-1} [41]. However, Al incorporation into the silica structure of the SBA-15 results in loss of microporosity, leading to a substantially mesoporous structure as evidenced by the type H1 hysteresis loop in the raw isotherm [42]. In turn, this results in lower total surface areas, in agreement with what was observed for the Al-SBA-15 catalyst in this work.

Table 2. Structural/textural and acidic properties of catalytic materials.

Catalyst	BET Surface Area (m^2 g^{-1})	Micropore Surface Area (m^2 g^{-1})	Micropore volume (cm^3 g^{-1})	Total pore volume (cm^3 g^{-1})	Mean pore diameter (nm)	Acidity (μmol g^{-1})
e-FCC	167	133	0.06	0.17	1.5	45
Al-SBA-15	414	0	0.00	0.91	6.8	564
ZSM-5	420	353	0.16	0.21	1.2	539

Comparing the porous properties (Table 2), ZSM-5 was a microporous material with relatively high micropore volume and micropore surface area, while Al-SBA-15 was a purely mesoporous material

with significantly higher total pore volume. The e-FCC catalyst also exhibited relatively high micropore surface area, contributing nearly to all of its total surface area, which was attributed to the FAU zeolite phase in the material. The mean pore diameters, calculated using the BJH method applied to the desorption branch of the isotherms, were expectedly different between the catalysts. Al-SBA-15 exhibited the largest mean pore diameter at 6.8 nm, with a narrow pore size distribution (see Fig. S1 in the supporting information). ZSM-5 and FAU zeolite (the zeolite type present in e-FCC) are known to have pore sizes of ca. 0.5 nm and ca. 0.7 nm, respectively [43].

The acidic properties of the catalysts were measured and quantified using propylamine-TPD and are also presented in Table 2. The ZSM-5 and Al-SBA-15 catalysts both displayed high and comparable acidity of 539 and 564 μmol g^{-1}, respectively. According to the literature, the quality of aluminium incorporation for the generation of Brønsted acid sites is highly dependent on the synthesis procedure [34]. The typical synthesis method of Al-SBA-15 is via direct synthesis, which is the direct mixing of silicon and aluminium precursors in the synthesis solution. However, this results in less control over the nature of the aluminium incorporation and achievable acidities range from 58 to 440 μmol g^{-1}, therefore much less than is typically displayed by zeolites [44,45]. The much higher acidity of the Al-SBA-15 produced in this paper indicated that the synthesis procedure employed (see Section 2.2) was effective for the incorporation of a substantial quantity of Al atoms in the tetrahedral environment in the structure of the material. As mentioned, the high acidity in both ZSM-5 and Al-SBA-15 is caused by framework aluminium and is responsible for catalysing a host of reactions such as cracking, deoxygenation and aromatization, which are prominent in catalytic fast pyrolysis [23,24]. In contrast, the e-FCC exhibited the lowest acidity at 45 μmol g^{-1}, which was expected considering its low surface area.

Although acid strength cannot be directly quantified using the propylamine-TPD method, the acid strength of the three catalysts can be compared using the temperature of peak propene desorption (Fig. 4). The greater the temperature of maximum propene desorption the weaker the acid strength due to the requirement of increased thermal energy to drive the reaction rate. The propene TPD profiles (Fig. 4) revealed two distinct peaks for ZSM-5 (T= 419 and 487 °C), indicative of two types of acid sites with different strengths. The type of site with the greatest acid strength, T= 419 °C, was around four times larger than the type of site with weaker strength, T= 487 °C. In contrast, both e-FCC and Al-SBA-15 had only one distinguishable peak at 430 °C and 441 °C, respectively. Therefore, together with the quantitative data, the Al-SBA-15 can be considered to display similar acidic properties to those found in zeolites.

Fig. 4. TPD profiles of reactively formed propene from propylamine decomposition over the e-FCC, ZSM-5 and Al-SBA-15 catalysts.

3.3 Micro-reactor experimental results

3.3.1 Non-catalytic pyrolysis of beech wood

The non-catalytic pyrolysis of beech wood at 500 °C decomposed the woody-biomass sample into a wide range of products. A comprehensive list of the detected products is included in Table S2 in the Supporting Information. It must be noted that the non-catalytic fast pyrolysis of beech wood typically yields a very complex mixture of volatiles composed of over 300 individual products [8]. Quantification of the most common 30 compounds, listed in Table S1, is consistent with previously reported data [46] and provided a baseline for the comparison with the catalytic pyrolysis results. The quantification results are presented in Table 3, where the condensable products were grouped into acids, alcohols, aldehydes, esters/ethers, monocyclic aromatic hydrocarbons, polyaromatic hydrocarbons, furans, phenolics and anhydrosugars for easier comprehension. A more detailed breakdown of the quantified condensable products is provided in the Supporting Information, in Table S2.

Table 3. Product distribution from the non-catalytic and in-situ catalytic pyrolysis of beech wood, at different catalyst to biomass ratios (C/B) and 500 °C (carbon yields, C %).

	No catalyst	e-FCC			Al-SBA-15			ZSM-5		
C/B		1:1	5:1	10:1	1:1	5:1	10:1	1:1	5:1	10:1
Acids	7.0 ±0.2	7.6 ±0.2	7.6 ±0.2	7.1 ±0.0	6.3 ±0.3	2.3 ±0.0	0.7 ±0.0	5.7 ±0.3	0.9 ±0.0	0.4 ±0.1
Alcohols	2.3 ±0.0	2.7 ±0.3	3.6 ±0.1	3.4 ±0.4	4.1 ±0.1	3.0 ±0.1	4.1 ±0.3	0.0 ±0.0	0.0 ±0.0	0.0 ±0.0
Aldehydes	7.3 ±0.2	6.9 ±0.4	3.5 ±1.9	1.6 ±0.0	1.5 ±0.1	0.0 ±0.0	0.0 ±0.0	1.2 ±0.0	0.0 ±0.0	0.0 ±0.0
Ester/Ethers	4.2 ±0.1	2.2 ±0.0	2.1 ±0.0	1.7 ±0.2	2.3 ±0.1	2.2 ±0.2	2.0 ±0.2	1.4 ±0.1	0.0 ±0.0	0.0 ±0.0
Aromatics[a]	0.0 ±0.0	0.0 ±0.0	0.04 ±0.0	0.05 ±0.0	0.0 ±0.0	0.5 ±0.0	0.7 ±0.1	2.0 ±0.1	13.9 ±0.5	15.7 ±0.5
PAHs	0.0 ±0.0	0.0 ±0.0	0.0 ±0.0	0.0 ±0.0	0.0 ±0.0	0.3 ±0.0	0.4 ±0.0	1.5 ±0.1	5.2 ±0.2	5.8 ±0.0
Furans	0.8 ±0.0	1.8 ±0.1	2.6 ±0.2	3.2 ±0.0	2.6 ±0.1	2.8 ±0.0	1.9 ±0.0	2.7 ±0.2	0.[illegible] 0.0	0.[illegible] ±0.0
Phenolics	2.4 ±0.1	2.6 ±0.1	2.4 ±0.1	1.8 ±0.1	1.4 ±0.1	0.1 ±0.0	0.0 ±0.0	2.9 ±0.[illegible]	0.[illegible] 0.0	0.1 ±0.0
Anhydrosugars	7.6 ±0.8	4.0 ±0.9	0.8 ±0.3	0.0 ±0.0	1.0 ±0.1	0.0 ±0.0	0.0 ±0.0	2.5 ±0.4	0.[illegible] 0.0	0.0 ±0.0
Total Gas	6.3 ±0.5	7.9 ±0.2	9.0 ±0.6	11.1 ±0.4	10.5 ±0.2	13.2 ±0.2	15.[illegible] ±0.[illegible]	15.[illegible] 0.2	22.8 ±0.6	25.1 ±1.5
CO	3.1 ±0.3	4.1 ±0.0	5.2 ±0.5	6.8 ±0.3	6.6 ±0.2	8.9 ±0.2	9.[illegible] ±0.[illegible]	9.7 ±0.1	14.2 ±0.2	15.6 ±0.8
CO_2	3.1 ±0.2	3.8 ±0.2	3.8 ±0.1	4.3 ±0.0	3.8 ±0.0	4.2 ±0.0	4.6 ±0.1	4.1 ±0.3	5.1 ±0.0	5.4 ±0.1
Ethene	0.0 ±0.0	0.0 ±0.0	0.0 ±0.0	0.0 ±0.0	0.0 ±0.[illegible]	0.[illegible] ±0.0	0.8 ±0.5	0.8 ±0.0	2.3 ±0.4	2.6 ±0.5
Propene	0.0 ±0.0	0.0 ±0.0	0.0 ±0.0	0.0 ±0.0	0.0 ±0.0	0.0 ±0.0	0.6 ±0.2	0.6 ±0.0	1.2 ±0.0	1.5 ±0.1
Char/Coke	19.8 ±1.6	29.5 ±2.0	28.0 ±3.7	27.3 ±[illegible]	4[illegible].1 ±2.7	47.5 ±6.2	40.3 ±5.1	32.5 ±8.4	33.7 ±7.2	35.6 ±2.9
Total	57.6	65.2	59.[illegible]	5[illegible].3	75.7	71.9	65.6	67.7	77.3	82.7

[a]Mono-cyclic aromatic hydrocarbons.

The three main product groups obtained from non-catalytic pyrolysis, on a C % basis, were acids (7%), aldehydes (7.3%) and anhydrosugars (7.6%). Acids were primarily composed of acetic acid; aldehydes were mainly composed of succindialdehyde and glycolaldehyde, in relatively equal proportions. Anhydrosugars were mostly composed of levoglucosan, the primary decomposition product of cellulose. Lower MW compounds, including alcohols, esters, ethers and furans, were produced in smaller quantities. A wide range of phenolic products were observed in relatively low concentrations and were primarily alkoxy-phenols, i.e. guaiacyl- and syringyl-type compounds that were derived from the decomposition of lignin.

The total gas yield for the non-catalytic run was 6.3 C %, with carbon ending up as both CO and CO_2 in equal proportions. The char/coke yields obtained by the non-catalytic pyrolysis of beech wood were consistent with the proximate analysis results obtained by thermogravimetric analysis (see Table 1)

and demonstrated that 19.8 C % (8.7 wt. %) of carbon in the feedstock was converted to fixed carbon. The total carbon yield from non-catalytic pyrolysis of beech wood was ca. 57.6 C %, which is relatively low. This was attributed to the fact that a significant portion of the products from the pyrolysis of lignocellulosic biomass are non-GC-detectable and could not be quantified [47].

3.3.2 Catalytic fast pyrolysis of beech wood

The catalytic fast pyrolysis of beech wood with ZSM-5, Al-SBA-15 and e-FCC was investigated at 500 °C and at three different C/B ratios; 1, 5 and 10:1. As discussed previously, the ZSM-5 and Al-SBA-15 catalysts had similar acidity and surface areas (see Table 2), enabling a close comparison between their catalytic activity. On the other hand, the e-FCC had significantly lower acidity and surface area, as explained earlier. This enabled a comparison of the products from CFP with two highly acidic catalysts (ZSM-5 and Al-SBA-15) and a typical industrial catalyst with significantly lower acidity and surface area (e-FCC).

One of the most notable observations was that all catalysts significantly increased the yields of gaseous products in the order of ZSM-5 > Al-SBA-15 > e-FCC, as can be seen in Fig. 5. The main gaseous products in all experiments were CO and CO_2. Notably, the CO:CO_2 ratio increased in all catalytic experiments, suggesting that the acidic catalysts primarily catalysed decarbonylation reactions, consistent with CFP studies at larger scales [18,48]. With the introduction of ZSM-5 at a C/B ratio of 1:1, total gas production was increased by approximately threefold in comparison to the non-catalytic pyrolysis. Notably, the production of alkenes, which is characteristic of extensive cracking reactions, was apparent from a low C/B ratio (1:1) in the case of ZSM-5.

Fig. 5. Comparison of carbon yields of non-condensable gaseous products from the non-catalytic and catalytic pyrolysis of beech wood at 500 °C. dZvµu(ƌoÁPZǒŜu]v]ǌ C/B ratio.

In comparison, alkenes in the case of the Al-SBA-15 catalyst were not detected until a C/B ratio of 10:1 was used. Moreover, the total gas yield with the Al-SBA-15 catalyst was markedly lower than with the ZSM-5, despite the similar acidity and surface area of both catalysts. This suggested that high acidity was not the only factor affecting the cracking and deoxygenation of the pyrolysis vapours; pore structure, acid site density (number of acid sites per unit of pore volume) and acid strength (see Fig. 4) possibly also played a significant role. Nonetheless, as previously stated, alkenes were not detected using e-FCC suggesting that the low acidity and surface area was still too low to produce the hydrocarbon gases.

All catalysts decreased the yield of levoglucosan, even at low C/B ratios. e-FCC decreased the yield of levoglucosan to approximately 4 C % from around 8 C %, while ZSM-5 decreased the yield to around 2.5 C %. Al-SBA-15 was the most effective catalyst for the degradation of levoglucosan and reduced the yield to approximately 1 C %. Levoglucosan is the primary decomposition product of cellulose and is a thermally stable intermediate. Cracking experiments at temperatures as high as 600 °C have displayed no subsequent degradation intermediates [49]. Therefore, in this work, the decomposition of levoglucosan was solely attributed to catalytic reactions and not to thermal cracking.

The kinetic diameter of levoglucosan is 0.67 nm [20], whereas the well-defined pore geometries of FAU (e-FCC) and MFI (ZSM-5) are ca. 0.7 nm [50] and ca. 0.5 x 0.5 nm [51], respectively. The N_2 physisorption measurements of the Al-SBA-15 catalyst showed that the catalyst exhibited a hexagonal cylindrical pore arrangement with a much larger mean pore diameter of approximately 7 nm (Table 2). Therefore, the diffusion of levoglucosan was most likely limited in ZSM-5, preventing its conversion on the majority of [illegible] acid sites. Instead, the catalytic degradation of levoglucosan most likely took place on the acid sites located on the external surface of the ZSM-5.

A combination of the acidity of the catalyst and the accessibility of the acid sites were key factors in the [illegible] levoglucosan conversion. This was evident as Al-SBA-15, with a similar acidity to ZSM-5, displayed increased conversion of levoglucosan at lower C/B ratios. In comparison, e-FCC had a much lower acidity and was significantly less effective for the conversion of levoglucosan. In the proposed mechanism of acid catalysed decomposition of levoglucosan by Lin et al. [52], levoglucosan is first decomposed through dehydration to other anhydro-monosaccharides such as levoglucosenone. Following this, the anhydro-monosaccharides are decomposed to form furanoses and a variety of fragmentation species such as glycolaldehyde and glyceraldehyde, through dehydration, decarbonylation, decarboxylation and retro/aldol condensation reactions.

The production of furanic compounds was increased by all three catalysts in comparison to the non-catalytic pyrolysis of beech wood (Table 3 and Fig. 6). This was attributed to the breakdown of levoglucosan, as described above, in addition to the cyclisation of hemicellulose intermediates [53].

The yield of furan products was increased at increasing C/B ratios using the e-FCC catalyst (Table 3). The highest yield of total furan products achieved by e-FCC was 3.2 C %. Similarly, high initial yields were evident in both ZSM-5 and Al-SBA-15, which supported the hypothesised furan formation mechanism via acid catalysed degradation of levoglucosan and hemicellulose. At increased C/B ratios of both ZSM-5 and Al-SBA-15 catalysts, the yield of total furans was reduced. Although, this was particularly evident by ZSM-5 compared to Al-SBA-15. This suggested that furans were intermediate catalytic products and were further converted to other compounds, or by-product coke and gas when more acid sites became available. Furthermore, the smaller pore size of ZSM-5 compared to Al-SBA-15 facilitated the conversion of furans at a higher rate.

The data on the yields of individual furan type products, provided in the supporting information (Table S2) shows there was variability across the three C/B ratios and across the three catalysts. This may provide mechanistic information on their formation and conversion. For example, as evident in Fig. 6, the yield of furfural initially increased using the e-FCC catalyst from 0.9 C % to 1.3 C % at C/B ratio of 1:1 and 5:1, respectively. At a C/B ratio of 10:1 of e-FCC, the yield of furfural is decreased in favour of the formation of furan. This suggests that furfural is probably decarbonylated to furan as the number of available acid sites increases.

Fig. 6. Comparison of yields of key products from the non-catalytic and catalytic pyrolysis of beech ÁdZvµuGoÁvPZšu]v] tes the C/B ratio.

A mechanism for the acid catalysed conversion of furfural to furan was proposed by Charoenwiangnuea et al. [54] and is depicted schematically in Fig. 7. A previous experimental investigation by Fanchiang and Lin [55], and a successive theoretical investigation over ZSM-5 by Charoenwiangnuea et al. [54], both proposed that furan is subsequently converted to intermediate products such as cyclohexene and 3,4-dimethylbenzaldehyde and then to higher aromatics in the pores of ZSM-5. This theory is supported by this study, with high initial yields of furan at 1:1 C/B ratio and a reduction in furan in favour of aromatics at higher C/B ratios.

Fig. 7. Proposed mechanism by Charoenwiangnuea et al. [54] for the acid catalysed conversion of furfural to furan and carbon monoxide.

The high yield of acidic products in fast pyrolysis liquid, in particular, acetic acid, is well-known and is responsible for its detrimental effects such as low stability and corrosiveness [7]. In this study, there was a high yield of acid products for the uncatalysed pyrolysis of beech wood. The yield of acidic products was increased slightly with the introduction of the e-FCC catalyst. This was attributed to the acid-catalysed cracking of biomass oligomers facilitated by e-FCC. In contrast, a significant reduction in the yield of acidic products was evidenced by both the Al-SBA-15 and ZSM-5 catalysts.

It was suggested by Corma et al. [56] that acetic acid is first converted to acetone and subsequently dehydrated to iso-butene. It is then further converted to aromatics, alkenes and coke in acidic catalysts, which is in agreement with our observations in the case of the ZSM-5 catalyst (see Table 3 and Fig. 6). However, the conversion of acetic acid by Al-SBA-15 did not result in the increase of significant yields of any identified compounds apart from non-condensable gases and coke. This was despite the fact that the Al-SBA-15 catalyst had very similar total surface area and acidity to the ZSM-5 catalyst (see Table 2). This suggested that the higher acid site density and the microporous shape-selective structure of the ZSM-5 were more important factors for the formation of desirable aromatic hydrocarbons (Fig. 8, acetic acid and toluene). The absence of these key shape-selective properties resulted in the conversion of the highly reactive biomass-derived compounds to coke and non-condensable gases, as was observed in the case of the Al-SBA-15 catalyst.

Fig. 8. Relationship between acetic acid, syringol, toluene and naphthalene 2-methyl and the number of acid sites in each experiment. The number of acid sites on the x axis were calculated as the mass of catalyst used in the reactor (g) multiplied by the catalyst acidity (μmol g^{-1}).

The yield of alkoxy-phenols was slightly increased for both e-FCC and ZSM-5, while the yield was reduced for Al-SBA-15 at the low C/B ratio, compared to the uncatalysed experiment (Fig. 6). In addition, the yield of alkylated phenols also increased at low C/B ratios for all catalysts compared to the uncatalysed experiment. However, for the two higher acidity catalysts, Al-SBA-15 and ZSM-5, the yield of alkylated phenols was reduced with increased C/B ratio. This effect was more pronounced in the case of the Al-SBA-15 catalyst. Considering the similar acidity and surface area, this was attributed to the lack of diffusional limitations of Al-SBA-15 compared to the ZSM-5 catalyst. Increasing the C/B ratio of these catalysts resulted in the complete elimination of alkoxy-phenols but also the reduction and eventual elimination of alkyl-phenols as well, which was advantageous in terms of oxygen rejection. On the other hand, in the case of the e-FCC catalyst, a notable increase of alkoxy-phenols was observed, accompanied by an increase in the yields of alkyl-phenols, which further increased with increasing C/B ratio. Based on these observations it can be concluded that the acid catalysts facilitated the decomposition of lignin-derived oligomers into alkoxy-phenolic products (Fig. 8, syringol). These further reacted on the acid sites to form deoxygenated alkyl-phenols, i.e. increased oxygen rejection.

Higher acid site availability by the introduction of more catalyst in the reactor (higher C/B ratios) resulted in the conversion of the alkyl-phenols to other products, such as aromatic hydrocarbons, non-condensable gases and coke.

Work by To and Resasco [57], on the conversion of low MW phenolic compounds over ZSM-5 and zeolite Y (FAU type), evidenced the conversion of phenolics to aromatics via the formation of a reactive phenolic pool. Furthermore, in their work, ZSM-5 showed better performance in terms of production of aromatics and increased resistance to deactivation than zeolite Y. However, it was observed that below 600 °C, a considerable proportion of the reactant phenolics and products became trapped inside the pores of the zeolites resulting in coke formation. This was due to the high adsorption capacity of the zeolites which led to increased coke yields due to entrapment within the pores. Increasing the temperature of their experiments resulted in the cracking of the adsorbed phenolics and the formation of aromatic hydrocarbons. Consequently, the yield of coke was also reduced.

Our results appear to be in disagreement with other work in terms of phenolic production where the CFP of biomass with mesoporous aluminosilicates was investigated. Work by Adam et al. [22] observed an increased yield (by up to 13.1 wt. %) of phenolic products compared to non-catalytic fast pyrolysis experiments. An increased yield (by 12.5 wt. %) of phenolic products was also noted by Triantafyllidis et al. [58] using Al-MCM-41. However, a sharp decrease in phenolic products down to 1.3 wt. % was observed using a mesoporous aluminosilicate with similar acidity to Al-MCM-41. In comparison to this study, the previously tested mesoporous catalysts are of much lower acidity compared to the Al-SBA-15 catalyst used in this work which could be the reason for the discrepancy in phenolic product formation. An increased yield of phenolic products was also evidenced by the low acidity e-FCC catalyst. At increased catalyst acidities it can be expected that a larger proportion of lignin will be cracked. In addition, the increased catalyst acidity will result in the conversion of phenolic products to alkyl-phenols and aromatics or coke. This was observed in this study with both Al-SBA-15 and ZSM-5 at higher C/B ratios.

As expected, the ZSM-5 catalyst was particularly effective for the formation of monoaromatic hydrocarbons. At the lowest C/B ratio (1:1), the monoaromatic hydrocarbons yield was ca. 2 C % yield and was significantly increased to nearly 14 C % at a 5:1 ratio. Interestingly, at 10:1 ratio there was only a relatively slight increase in aromatics and that was not proportional to the increased C/B ratio. This suggests that there is an optimum ZSM-5 C/B ratio for the formation of aromatic hydrocarbons.

As discussed earlier, despite the similar acidity and surface area of the Al-SBA-15 and ZSM-5 catalysts, Al-SBA-15 produced a lower quantity of aromatics compared to ZSM-5. It was hypothesised the combination of large pore volume and a high number of acid sites facilitated the repolymerization of the highly reactive biomass-derived products to large, high molecular weight products and eventually

to coke [59]. e-FCC produced a very small quantity of aromatics (< 0.05 C %), even when high C/B ratios were employed. The low yield was attributed to the low acidity and low surface area of the catalyst.

An almost linear trend is evident between the formation of monocyclic aromatics (BTX) and PAHs in ZSM-5. As previously mentioned, this suggested an inefficient diffusion of the monocyclic aromatics out of the pore network of the ZSM-5, allowing excessive aromatisation reactions to take place. However, even considering this, the ZSM-5 exhibited superior performance compared the Al-SBA-15 in terms of limiting excessive aromatization reactions for the formation of bulky PAH products. Even though the overall yield of aromatics produced by Al-SBA-15 was significantly lower, the ratio of PAHs to monocyclic aromatics was substantially greater in the case of Al-SBA-15 (0.64) than in the case of ZSM-5 (0.37). This again can be attributed to the larger pore size of Al-SBA-15 compared to ZSM-5.

The larger pore size of Al-SBA-15 resulted in enhanced product and reactant diffusion, however, due to the large available pore space, it also readily allowed the formation of higher MW PAHs. This was further supported by the fact that lower MW PAHs, such as naphthalene and naphthalene 2-methyl, were formed in ZSM-5 in higher proportions due to the restricted pore space (Fig. 8, naphthalene 2-methyl). In contrast, Al-SBA-15 produced a larger proportion of higher MW PAHs, such as anthracenes. These contributed to 52 % of overall PAHs compared to 7 % in ZSM-5. It is therefore evident that both ZSM-5 and Al-SBA-15 catalysed aromatization reactions, however, the absence of micropores in Al-SBA-15 resulted in excessive aromatization and the formation of some high molecular weight PAHs and coke (discussed later).

The coking and subsequent deactivation of the catalyst is one of the major factors that impact the economic feasibility of many biomass catalytic upgrading procedures, including catalytic fast pyrolysis [60]. The effect of coking can be managed in CFP using circulating fluidised bed reactor designs, whereby coke burning for the regeneration of the catalyst also provides the process with heat. However, the main problem with coking is the carbon loss from the liquid product resulting in an unfavourable high O/C ratio and lower liquid product yield. Therefore, the minimisation of coke yields while maintaining high levels of catalytic activity is essential for future catalyst design.

Coke is mainly formed on the active acid sites and is produced by several mechanisms such as condensation and hydrogen transfer [61]. Moreover, so-called coke-precursors, often oxygenated hydrocarbons such as phenolics, and the products of the polymerisation of mono and polycyclic aromatic hydrocarbons, are notorious for favouring the production of coke [62,63]. In the catalytic fast pyrolysis experiments, it can be expected that char yields remain relatively constant. Therefore, any significant increase in the char/coke yields can be attributed to catalytically formed coke on the

surface of the catalyst. The results show that there was a significant increase in the char/coke yields in the catalytic experiments compared to the non-catalytic experiment (char yield 19.8 C %, Table 3).

In the catalytic experiments, ZSM-5 produced char/coke yields in the range of ca. 32 to 36 C %. The char/coke yields increased slightly with increasing C/B but overall remained relatively stable. Al-SBA-15 produced considerably higher yields of coke in the range of ca. 40 C % and 48 C %. The mesoporous nature of the Al-SBA-15 proved to be favourable for coke formation, compared to ZSM-5, by providing more space for coke precursors to form and polymerise. On the other hand, the microporous pore geometries of ZSM-5 restricted the formation of undesirable coke by preventing the repolymerisation of oxygenates and other compounds. e-FCC exhibited the lowest char/coke yield among all three catalysts (27-30 C %), which was attributed to its low overall activity. The char/coke yields produced by e-FCC remained relatively stable with increased C/B ratios and displayed lower standard deviation between experiments.

The high standard deviation of the char/coke yields was notable and indicated the low accuracy of the experimental method used to determine the solid product yields. However, despite the significant variance between the char/coke yield results, there were no other products observed by GC-MS. Therefore, it is reasonable to assume that any increase in mass was due to catalytically formed coke.

4 Conclusions

In this work, a high acidity mesoporous Al-SBA-15 catalyst was synthesised utilizing an enhanced aluminium incorporation strategy to obtain a material with high aluminium content in tetrahedral environment. The synthesized Al-SBA-15 catalyst was shown to possess comparable acidity to that of a commercial crystalline ZSM-5 zeolite with a SiO_2/Al_2O_3 ratio of 30. The two catalysts, along with a typical industrial fluid catalytic cracking catalyst (e-FCC) with lower acidity, were compared for the catalytic fast pyrolysis of beech wood in a micropyrolyser. All three catalysts were employed at three different catalyst to biomass (C/B) ratios, to investigate the selectivity of the catalysts across varying concentrations of acid sites in the reactor.

Regardless of catalyst structure, all three solid acid catalysts displayed similar reaction pathways for the initial conversion of the primary biomass decomposition products, such as the cracking of larger intermediates, levoglucosan and hemicellulose components to produce furans and other oxygenates, as well as the cracking of lignin oligomers to produce alkoxy-phenols. As the concentration of acid sites in the reactor increased, catalyst structure became a determining factor for the conversion of the cracked intermediates into desirable products. In the case of the ZSM-5 catalyst intermediate oxygenates were converted to deoxygenated products such as desirable monoaromatic hydrocarbons and PAHs. In the case of the Al-SBA-15 catalyst, minimal yields of desirable products were observed,

while high yields of solid byproduct were obtained. Since both catalysts had very similar surface area and acidity, the difference in their selectivity was attributed to their porous structure. While the mesopores and high acidity of the Al-SBA-15 catalyst were effective for the initial conversion of the primary biomass decomposition products, the ZSM-5 shape-selective micropores proved to be more effective for the conversion of intermediate oxygenates into desirable products and the suppression of solid byproduct formation.

Previous comparisons of Al-SBA-15 and ZSM-5 catalysts for the conversion of biomass pyrolysis vapours utilised low acidity Al-SBA-15 catalysts, which were not as selective as ZSM-5 catalysts for the formation of desirable aromatic hydrocarbons. This work showed that increasing the acidity of the Al-SBA-15 to levels comparable to ZSM-5 catalysts did not lead to comparable selectivity to desirable compounds and further highlighted the importance of catalyst shape-selectivity for the conversion of pyrolysis vapours into desirable products and the suppression of undesirable solid product formation.

Acknowledgements

Joseph Socci would like to thank the Society of Chemical Industry (SCI) for providing a Messel Travel Bursary and Aston University for funding his PhD scholarship. The authors would also like to thank Dr. Amin Osatiashtiani for his assistance with TGA-MS.

References

[1] F. Schiefelbein G, J. Sealock L, S. Ergu Thermochemical Conversion of Biomass to Fuels and Feedstocks: An Overview of R&D Activit Funded by the Department of Energy, in: Therm. Convers. Solid Wastes Biomass, 1980: pp. 1 26. doi:doi:10.1021/bk-1980-0130.ch002.

[2] A. V. Bridgwater, Review of fast pyrolysis of biomass and product upgrading, Biomass and Bioenergy. 38 (2012) 68t 94. doi 0.10 6/j.biombioe.2011.01.048.

[3] G.W. Huber, S. Iborra, A. Corma, Synthesis of transportation fuels from biomass: Chemistry, catalysts, and engineering, Chem. Rev. 106 (2006) 4044t 4098. doi:10.1021/cr068360d.

[4] R.A. Sheldon, Green and sustainable manufacture of chemicals from biomass: state of the art, Green Chem. 16 (2014) 9 0t 963. doi:10.1039/C3GC41935E.

[5] C.A. Mullen, A. Boateng, Chemical Composition of Bio - oils Produced by Fast Pyrolysis of Two Energy Crops, Energy & Fuels. 22 (2008) 2104t 2109. doi:10.1021/ef700776w.

[6] S.W. Banks, D. Nowakowski, A. V Bridgwater, Impact of Potassium and Phosphorus in Biomass on the Properties of Fast Pyrolysis Bio-oil, Energy & Fuels. (2016) 8009t 8018. doi:10.1021 acs.energyfuels.6b01044.

[7] S. Czernik, A. V. Bridgwater, Overview of applications of biomass fast pyrolysis oil, Energy and Fuels. 18 (2004) 590t 598. doi:10.1021/ef034067u.

[8] P.M. Mortensen, J.D. Grunwaldt, P.A. Jensen, K.G. Knudsen, A.D. Jensen, A review of catalytic upgrading of bio-oil to engine fuels, Appl. Catal. A Gen. 407 (2011) 1t 19. doi:10.1016/j.apcata.2011.08.046.

[9] M.W. Nolte, A. Saraeian, B.H. Shanks, Hydrodeoxygenation of cellulose pyrolysis model compounds using molybdenum oxide and low pressure hydrogen, Green Chem. 19 (2017) 3654t 3664. doi:10.1039/c7gc01477e.

[10] C. Liu, H. Wang, A.M. Karim, J. Sun, Y. Wang, Catalytic fast pyrolysis of lignocellulosic biomass, Chem. Soc. Rev. 43 (2014) 7594t 7623. doi:10.1039/C3CS60414D.

[11] S.D. Stefanidis, K.G. Kalogiannis, A.A. Lappas, Co-processing bio-oil in the refinery for drop-in biofuels via fluid catalytic cracking, Wiley Interdiscip. Rev. Energy Environ. 7 (2018) e281. doi:10.1002/wene.281.

[12] M.S. Talmadge, R.M. Baldwin, M.J. Biddy, R.L. McCormick, G.T. Beckham, G.A. Ferguson, S. Czernik, K.A. Magrini-Bair, T.D. Foust, P.D. Metelski, C. Hetrick, M.R. Nimlos, A perspective on oxygenated species in the refinery integration of pyrolysis oil, Green Chem. 16 (2014) 407t 453. doi:10.1039/c3gc41951g.

[13] B. Zhang, Z.-P. Zhong, X.-B. Wang, K. Ding, Z.-W. Song, Catalytic upgrading of fast pyrolysis biomass vapors over fresh, spent and regenerated ZSM-5 zeolites, Fuel Process. Technol. 138 (2015) 430t 434. doi:10.1016/j.fuproc.2015.06.011.

[14] D.J. Mihalcik, C.A. Mullen, A.A. Boateng, Screening acidic zeolites for catalytic fast pyrolysis of biomass and its components, J. Anal. Appl. Pyrolysis. 92 (2011) 224t 232. doi:10.1016/j.jaap.2011.06.001.

[15] F. Ronsse, K.M. Van Geem, R. Van Duren, G. Yildiz, F. Ronsse, J. Vercruysse, J. Daels, H.E. Toraman, K.M. van Geem, G.B. Marin, R. van Duren, W. Prins, In situ performance of various metal doped catalysts in micro-pyrolysis and continuous fast pyrolysis, Fuel Process. Technol. 144 (2016) 312t 322. doi:10.1016/j.fuproc.2016.01.012.

[16] E.F. Iliopoulou, E. V. Antonakou, S.A. Karakoulia, I.A. Vasalos, A.A. Lappas, K.S. Triantafyllidis, Catalytic conversion of biomass pyrolysis products by mesoporous materials: Effect of steam stability and acidity of Al-MCM-41 catalysts, Chem. Eng. J. 134 (2007) 51t 57. doi:10.1016/j.cej.2007.03.066.

[17] M.I. Nokkosmäki, E.T. Kuoppala, E. a. Leppämäki, a. O.I. Krause, Catalytic conversion of biomass pyrolysis vapours with zinc oxide, J. Anal. Appl. Pyrolysis. 55 (2000) 119t 131. doi:10.1016/S0165-2370(99)00071-6.

[18] S.D. Stefanidis, K.G. Kalogiannis, E.F. Iliopoulou, A.A. Lappas, P.A. Pilavachi, In-situ upgrading of biomass pyrolysis vapors: catalyst screening on a fixed bed reactor, Bioresour. Technol. 102 (2011) 8261t 7. doi:10.1016/j.biortech.2011.06.032.

[19] T.R. Carlson, J. Jae, Y.-C. Lin, G.A. Tompsett, G.W. Huber, Catalytic fast pyrolysis of glucose with HZSM-5: The combined homogeneous and heterogeneous reactions, J. Catal. 270 (2010) 110t 124. doi:10.1016/j.jcat.2009.12.013.

[20] J. Jae, G.A. Tompsett, A.J. Foster, K.D. Hammond, S.M. Auerbach, R.F. Lobo, G.W. Huber, Investigation into the shape selectivity of zeolite catalysts for biomass conversion, J. Catal. 279 (2011) 257t 268. doi:10.1016/j.jcat.2011.01.019.

[21] M. Kruk, M. Jaroniec, Y. Sakamoto, O. Terasaki, R. Ryoo, C.H. Ko, Determination of Pore Size and Pore Wall Structure of MCM-41 by Using Nitrogen Adsorption, Transmission Electron Microscopy, and X-ray Diffraction, J. Phys. Chem. B. 104 (2000) 292t 301. doi:10.1021/jp992717y.

[22] J. Adam, E. Antonakou, A. Lappas, M. Stöcker, M.H. Nilsen, A. Bouzga, J.E. Hustad, G. Øye, In situ catalytic upgrading of biomass derived fast pyrolysis vapours in a fixed bed reactor using mesoporous materials, Microporous Mesoporous Mater. 96 (2006) 93t 101. doi:10.1016/j.micromeso.2006.06.021.

[23] M.-J. Jeon, J.-K.K. Jeon, D.J. Suh, S.H. Park, Y.J. Sa, S.H. Joo, Y.-K.K. Park, Catalytic pyrolysis of biomass components over mesoporous catalysts using Py-GC/MS, Catal. Today. 204 (2013) 170t 178. doi:10.1016/j.cattod.2012.07.039.

[24] V.B.F. Custodis, S.A. Karakoulia, K.S. Triantafyllidis, J.A. Van Bokhoven, Catalytic Fast Pyrolysis of Lignin over High-Surface-Area Mesoporous Aluminosilicates: Effect of Porosity and Acidity, ChemSusChem. 9 (2016) 1134t 1145. doi:10.1002/cssc.201600105.

[25] Q. Lu, X. Zhu, W. Li, Y. Zhang, D. Chen, On-line catalytic upgrading of biomass fast pyrolysis products, Chinese Sci. Bull. 54 (2009) 1941t 1948. doi:10.1007/s11434-009-0273-5.

[26] L. Qiang, L. Wen-zhi, Z. Dong, Z. Xi-feng, Analytical pyrolysis-gas chromatography/mass spectrometry (Py-GC/MS) of sawdust with Al/SBA-15 catalysts, J. Anal. Appl. Pyrolysis. 84 (2009) 131t 138. doi:10.1016/j.jaap.2009.01.002.

[27] E. Yaman, A.S. Yargic, N. Ozbay, B.B. Uzun, K.G. Kalogiannis, S.D. Stefanidis, E.P. Pachatouridou,

E.F. Iliopoulou, A.A. Lappas, Catalytic upgrading of pyrolysis vapours: Effect of catalyst support and metal type on phenolic content of bio-oil, J. Clean. Prod. 185 (2018) 52t61. doi:10.1016/J.JCLEPRO.2018.03.033.

[28] K. Wang, J. Zhang, B.H. Shanks, R.C. Brown, Catalytic conversion of carbohydrate-derived oxygenates over HZSM-5 in a tandem micro-reactor system, Green Chem. 17 (2015) 557t564. doi:10.1039/c4gc01784f.

[29] F. Berruti, A.G. Liden, D.S. Scott, Measuring and modelling residence time distribution of low density solids in a fluidized bed reactor of sand particles, Chem. Eng. Sci. 43 (1988) 739t748. doi:10.1016/0009-2509(88)80068-X.

[30] T.C. Hoff, M.J. Holmes, J. Proano-Aviles, L. Emdadi, D. Liu, R.C. Brown, J.-P. Tessonnier, Decoupling the Role of External Mass Transfer and Intracrystalline Pore Diffusion on the Selectivity of HZSM-5 for the Catalytic Fast Pyrolysis of Biomass, ACS Sustain. Chem. Eng. 5 (2017) 8766t8776. doi:10.1021/acssuschemeng.7b01578.

[31] M.B. Shemfe, S. Gu, P. Ranganathan, Techno-economic performance analysis of biofuel production and miniature electric power generation from biomass fast pyrolysis and bio-oil upgrading, Fuel. 143 (2015) 361t372. doi:10.1016/j.fuel.2014.11.078.

[32] E.T.C. Vogt, B.M. Weckhuysen, Fluid catalytic cracking: recent developments on the grand old lady of zeolite catalysis, Chem. Soc. Rev. 7342 (2015) 7342t7370. doi:10.1039/c5cs00376h.

[33] S. Wu, Y. Han, Y.C. Zou, J.W. Song, L. Zhao, Y. Di, S.Z. Liu, F.S. Xiao, Synthesis of Heteroatom Substituted SBA-íñ Ç‰ -iµ]vP_DZU ZuX DE(íõ t492. doi:10.1021/cm0343857.

[34] A. Ungureanu, B. Dragoi, V. Hulea, T. Cacciaguerra, D. Meloni, V. Solinas, E. Dumitriu, Effect of oµu]v]µu]vÇ‰ -iµ]vPuZÇoEU]]vö properties of mesoporous SBA-15, Microporous Mesoporous Mater. 163 (2012) 51t64. doi:10.1016/j.micromeso.2012.05.007.

[35] T.J.G. Kofke, R.J. Gorte, W.E. Farneth, Stoichiometric adsorption complexes in H-ZSM-5, J. Catal. 114 (1988) 34t45. doi:10.1016/0021-9517(88)90006-1.

[36] A. Saraeian, M.W. Nolte, B.H. Shanks, Deoxygenation of biomass pyrolysis vapors: Improving clarity on the fate of carbon, Renew. Sustain. Energy Rev. 104 (2019) 262t280. doi:10.1016/j.rser.2019.01.037.

[37] L. Ye, Y. Xiping, Z. Yuxia, Y. Aidi, Test Method for Specific Surface Area of FCC Catalyst, ACTA Pet. Sin. 33 (2017) 1053t1060. doi:10.3969/J.ISSN.1001-8719.2017.06.003.

[38] A. Osatiashtiani, B. Puértolas, C.C.M. Oliveira, J.C. Manayil, B. Barbero, M. Isaacs, C. Michailof, E. Heracleous, J. Pérez-Ramírez, A.F. Lee, K. Wilson, On the influence of Si:Al ratio and hierarchical porosity of FAU zeolites in solid acid catalysed esterification pretreatment of bio-oil, Biomass Convers. Biorefinery. 7 (2017) 331t342. doi:10.1007/s13399-017-0254-x.

[39] K.S.W. Sing, Reporting physisorption data for gas/solid systems with special reference to the determination of surface area and porosity (Provisional), Pure Appl. Chem. 54 (1982) 22t22. doi:10.1351/pac198254112201.

[40] M. Zhang, F.L.P. Resende, A. Moutsoglou, Catalytic fast pyrolysis of aspen lignin via Py-GC/MS, Fuel. 116 (2014) 358t369. doi:10.1016/j.fuel.2013.07.128.

[41] Y. Wan, D. Zhao, On the controllable soft-templating approach to mesoporous silicates, Chem. Rev. 107 (2007) 2821t2860. doi:10.1021/cr068020s.

[42] J. Socci, A. Osatiashtiani, G. Kyriakou, T. Bridgwater, The catalytic cracking of sterically challenging plastic feedstocks over high acid density Al-SBA-15 catalysts, Appl. Catal. A Gen. 570 (2019) 218t227. doi:10.1016/J.APCATA.2018.11.020.

[43] S. Storck, H. Bretinger, W.F. Maier, Characterization of micro- and mesoporous solids by physisorption methods and pore-size analysis, Appl. Catal. A Gen. 174 (1998) 137t146. doi:10.1016/S0926-860X(98)00164-1.

[44] S. Xing, P. Lv, J. Fu, J. Wang, P. Fan, L. Yang, Z. Yuan, Direct synthesis and characterization of pore-broadened Al-SBA-15, Microporous Mesoporous Mater. 239 (2017) 316t327. doi:10.1016/j.micromeso.2016.10.018.

[45] P. Bhange, D.S. Bhange, S. Pradhan, V. Ramaswamy, Direct synthesis of well-ordered

mesoporous Al-SBA-15 and its correlation with the catalytic activity, Appl. Catal. A Gen. 400 (2011) 176t184. doi:10.1016/j.apcata.2011.04.031.

[46] A.M. Azeez, D. Meier, urgen Odermatt, T. Willner, J. Odermatt, T. Willner, Fast Pyrolysis of African and European Lignocellulosic Biomasses Using Py-GC/MS and Fluidized Bed Reactor, J. Anal. Appl. Pyrolysis. 24 (2010) 2078t2085. doi:10.1021/ef9012856.

[47] G. Lyu, S. Wu, H. Zhang, Estimation and Comparison of Bio-Oil Components from Different Pyrolysis Conditions, Front. Energy Res. 3 (2015) 28. doi:10.3389/fenrg.2015.00028.

[48] S. Vitolo, B. Bresci, M. Seggiani, M.G. Gallo, Catalytic upgrading of pyrolytic oils over HZSM-5 zeolite: Behaviour of the catalyst when used in repeated upgrading-regenerating cycles, Fuel. 80 (2001) 17t26. doi:10.1016/S0016-2361(00)00063-6.

[49] X. Chen, Y. Chen, Z. Chen, D. Zhu, H. Yang, P. Liu, T. Li, H. Chen, Catalytic fast pyrolysis of cellulose to produce furan compounds with SAPO type catalysts, J. Anal. Appl. Pyrolysis. 129 (2018) 53t60. doi:10.1016/j.jaap.2017.12.004.

[50] L.B. McCusker, D.H. Olson, C. Baerlocher, Atlas of Zeolite Framework Types, 2007. doi:10.1016/B978-0-444-53064-6.X5186-X.

[51] D.H. Olson, G.T. Kokotallo, S.L. Lawton, Meler, Crystal Structure and Structure-Related Properties of ZSM-5, J. Phys. Chem. 85 (1981) 2238t2243.

[52] Y.C. Lin, J. Cho, G.A. Tompsett, P.R. Westmoreland, G.W. Huber, Kinetics and mechanism of cellulose pyrolysis, J. Phys. Chem. C. 113 (2009) 20097t20107. doi:10.1021/jp9027025.

[53] S. rong Wang, T. Liang, B. Ru, X. juan Guo, Mechanism of xylan pyrolysis by Py-GC/MS, Chem. Res. Chinese Univ. 29 (2013) 782t787. doi:10.1007/s40242-013-2447-6.

[54] P. Charoenwiangnuea, T. Maihom, P. Kongpracha, J. Sirijaraensre, J. Limtrakul, Adsorption and decarbonylation of furfural over H-ZSM-5 zeolite: A DFT study, RSC Adv. 6 (2016) 105888t105894. doi:10.1039/c6ra24631a.

[55] W.L. Fanchiang, Y.C. Lin, Catalytic fast pyrolysis of furfural over H-ZSM-5 and Zn/H-ZSM-5 catalysts, Appl. Catal. A Gen. 419t420 (2012) 102t110. doi:10.1016/j.apcata.2012.01.017.

[56] X[illegible]sing biomass-derived oxygenates in the oil refinery: Catalytic cracking (FCC) reaction pathways and role of catalyst, J. Catal. 247 (2007) 307t327. doi:10.1016/j.jcat.2007.01.023.

[57] A.T. To, D.E. Resasco, Role of a phenolic pool in the conversion of m-cresol to aromatics over HY and HZSM-5 zeolites, Appl. Catal. A Gen. 487 (2014) 62t71. doi:10.1016/j.apcata.2014.09.006.

[58] K.S. Triantafyllidis, E.F. Iliopoulou, E. V. Antonakou, A.A. Lappas, H. Wang, T.J. Pinnavaia, Hydrothermally stable mesoporous aluminosilicates (MSU-S) assembled from zeolite seeds as catalysts for biomass pyrolysis, Microporous Mesoporous Mater. 99 (2007) 132t139. doi:10.1016/j.micromeso.2006.08.019.

[59] P.A. Horne, P.T. Williams, Reaction of oxygenated biomass pyrolysis model compounds over a ZSM-5 catalyst, Renew. Energy. 7 (1996) 131t144. doi:10.1016/0960-1481(96)85423-1.

[60] a. G. Gayubo, B. Valle, a. T. Aguayo, M. Olazar, J. Bilbao, Pyrolytic lignin removal for the valorization of biomass pyrolysis crude bio-oil by catalytic transformation, J. Chem. Technol. Biotechnol. 85 (2010) 132t144. doi:10.1002/jctb.2289.

[61] S. Müller, Y. Liu, M. Vishnuvarthan, X. Sun, A.C. van Veen, G.L. Haller, M. Sanchez-Sanchez, J. a. Lercher, Coke formation and deactivation pathways on H-ZSM-5 in the conversion of methanol to olefins, J. Catal. 325 (2015) 48t59. doi:10.1016/j.jcat.2015.02.013.

[62] A.J. Foster, J. Jae, Y.-T. Cheng, G.W. Huber, R.F. Lobo, Optimizing the aromatic yield and distribution from catalytic fast pyrolysis of biomass over ZSM-5, Appl. Catal. A Gen. 423t424 (2012) 154t161. doi:10.1016/j.apcata.2012.02.030.

[63] H.J. Park, H.S. Heo, J.-K. Jeon, J. Kim, R. Ryoo, K.-E. Jeong, Y.-K. Park, Highly valuable chemicals production from catalytic upgrading of radiata pine sawdust-derived pyrolytic vapors over mesoporous MFI zeolites, Appl. Catal. B Environ. 95 (2010) 365t373. doi:10.1016/J.APCATB.2010.01.015.